Liquid Crystals

Publication details, including instructions for authors and subscription information:
http://www.informaworld.com/smpp/title~content=t713926090

Dielectric versus optical response of chevron ferroelectric liquid crystals

W. Jeżewski[a]; W. Kuczyński[a]; J. Hoffmann[a]
[a] Polish Academy of Sciences, Institute of Molecular Physics, 60-179 Poznań, Poland

To cite this Article Jeżewski, W. , Kuczyński, W. and Hoffmann, J.(2007) 'Dielectric versus optical response of chevron ferroelectric liquid crystals', Liquid Crystals, 34: 11, 1299 — 1306

To link to this Article: DOI: 10.1080/02678290701602926

URL: http://dx.doi.org/10.1080/02678290701602926

Liquid Crystals, Vol. 34, No. 11, November 2007, 1299–1306

Dielectric versus optical response of chevron ferroelectric liquid crystals

W. JEŻEWSKI*, W. KUCZYŃSKI and J. HOFFMANN
Polish Academy of Sciences, Institute of Molecular Physics, Smoluchowskiego 17, 60-179 Poznań, Poland

(*Received 16 March 2007; accepted in final form 4 July 2007*)

Dielectric and optical methods to investigate the response of surface-stabilized ferroelectric liquid crystals (SSFLCs) of the chevron structure are examined and compared in the case of the azimuthal mode of collective relaxation processes. It is found that the variation of an effective (averaged over the chevron cell volume) dielectric permittivity tensor under the influence of a weak alternating external electric field is approximately equivalent to the transformation of this tensor as a consequence of the rotation of the laboratory frame around the axis perpendicular to the smectic plane about a small angle. Then, using an analytic solution of the equation of motion describing the azimuthal rotation of molecules, it is shown that both of the analysed approaches to calculate and measure the response of SSFLCs yield consistent results for these rotational dynamic processes. This allows the calculation of the spontaneous polarization of the unit volume of chevron slabs, provided that the pretilted azimuthal angle (in the absence of an applied electric field) within the smectic plane is known.

1. Introduction

Dielectric and optical response methods are the main approaches in the investigation of ferroelectric modes in liquid crystals [1–3]. In general, however, these methods are not equivalent, at least for some finite ranges of frequencies of an applied electric field. In particular, optical measurement results exhibit the existence of ionic currents at much lower field frequencies than the corresponding dielectric experimental results [3]. Thus, in contrast to the optical method, the dielectric method is capable of detecting such currents at relatively large field frequencies. Furthermore, the degree of possible coincidence of experimental data obtained by using the two methods for the same response modes depends on specific molecular alignment geometries of liquid-crystal systems. The problem of the consistency of dielectric and optical responses has been studied in detail, both experimentally and theoretically, in the case of systems with helical ordering [1, 2]. As has been demonstrated, the coincidence of the optical with the dielectric response approximately takes place for Goldstone and soft modes corresponding to small helical structure deformations, induced by a weak alternating field. This is due to the occurrence of the uniaxial symmetry of the effective permittivity tensor averaged over the sample volume, in the absence of the applied field, and also due to the equivalence of a weak field induced inclination of the optical axis to a rotation of the laboratory frame around the axis parallel to the smectic plane and to boundary plates, about a small angle. In the case of surface-stabilized ferroelectric liquid crystals (SSFLCs) with chevron structure, the correspondence between both types of dielectric response has not yet been analysed completely. Several experimental results have been reported, and these display good consistency for a wide range of field frequencies, apart from a low-frequency region for which ionic currents have a strong affect only on the dielectric response [3].

In this paper, the optical response associated with azimuthal excitations of molecules caused by weak electric fields in ferroelectric cells with the chevron structure is studied theoretically and experimentally. In contrast to systems with helical structure, the effective permittivity tensor (averaged over the entire sample volume) does not have a uniaxial symmetry for chevron-like SSFLCs in the absence of the external electric field, even in the limit case when smectic layers are not slanted (i.e. when they are perpendicular to boundary plates). However, it is found here that, similarly to systems with helical structures, a modification of this effective tensor resulting from a distortion of the molecular configuration under the influence of a weak applied electric field can nearly be identified with a transformation resulting from a slight rotation of the

---

*Corresponding author. Email: jezewski@ifmpan.poznan.pl

Liquid Crystals
ISSN 0267-8292 print/ISSN 1366-5855 online © 2007 Taylor & Francis
http://www.tandf.co.uk/journals
DOI: 10.1080/02678290701602926

laboratory frame around one axis, normal to the smectic plane. This immediately implies the correspondence of general functional forms of the frequency dependence of both responses of chevron SSFLCs. The correspondence is also verified by the dependence of the optical response on the dielectric response, determined experimentally for a wide range of field frequencies. It is also shown that the ratio of the dielectric response function to the optical response function involves only the local spontaneous polarization (per unit volume of a chevron slab), the unperturbed (in the absence of the electric field) azimuthal angle in the smectic plane and the amplitude of the modulation of passing light.

2. Chevron alignment geometry and the azimuthal molecular dynamics

Thin ferroelectric liquid crystal (FLC) systems stabilized by relatively strong interactions with boundary plates can form smectic layers with uniform chevroned structures [4–6]. A schematic illustration of such systems is presented in figure 1, where the molecular ordering is shown in two planes. Collective motions of molecules in chevron cells are usually investigated by analysing fluctuations of the azimuthal angle ϕ in the smectic plane (X–Y), along the X axis (normal to boundary surfaces). In the presence of an external electric field, applied along the X axis and sinusoidally alternating with the frequency ω, fluctuations of the azimuthal angle are described by the following dynamic field equation [7]

$$\frac{\partial^2\phi}{\partial x^2} - \gamma\frac{\partial\phi}{\partial t} = A\sin\phi\cos\omega t, \tag{1}$$

where $\gamma = \gamma_\phi/K$ and $A = P_S E$ with γ_ϕ, K, P_S and E denoting the azimuthal viscosity, the twist elastic constant, the local spontaneous polarization and the amplitude of the applied electric field, respectively. Clearly, boundary conditions taken to solve (1) should properly reflect the behaviour of molecules both at border surfaces and at the interface plane (see figure 1) [8–10]. This, however, involves using additional material constants that are, in general, unknown. To remedy the resulting intricacy, their number has been reduced by assuming that polar anchoring interactions can be ignored and by assuming that the azimuthal orientation of molecules at the interface plane does not depend on the applied electric field [7, 11]. Evidently, the first assumption is rather uncontrollable, while the second is even unphysical. Therefore, the solution for ϕ will be applied below in a form derived with the use of more realistic boundary conditions [12]. These conditions employ both non-polar and polar anchoring surface interactions and allow the molecules at the interface plane to follow the external electric field. Anchoring energies of molecules at sample surfaces (at $x = \pm d/2$ with d being the cell thickness) are taken here in a standard form [8, 10, 13]

$$W_\pm(\phi) = -\gamma_1\cos^2(\phi \pm \phi_0) \pm \gamma_2\cos(\phi \pm \phi_0), \tag{2}$$

where the convention that + and − refer to upper and lower chevron slabs, respectively, is used, γ_1 and γ_2 are the non-polar and polar surface energy strengths, respectively, and $\pm\phi_0$ denotes values of the pretilted azimuthal angle (in the upper and lower chevron slabs, respectively), in the absence of the applied electric field (see figure 1). Then, the boundary conditions for the angle ϕ at sample surfaces are determined near its zero-field equilibrium values by [12]

$$\frac{\partial}{\partial x}\phi_\pm\left(x = \pm\frac{d}{2}\right) \approx \pm v_\pm\left[\phi_\pm\left(x = \pm\frac{d}{2}\right) \pm \phi_0\right], \tag{3}$$

where $v_\pm = 2\lambda_1 \mp \lambda_2$ with $\lambda_1 = \gamma_1/K$ and $\lambda_2 = \gamma_2/K$. Moreover, for weak applied fields and for strong surface anchoring interactions, one can assume that molecular orientations at border plates and at the interface plane are identical [9, 10]. Then, one has

$$\phi_\pm\left(\frac{d}{2}\right) = \phi_\pm(0). \tag{4}$$

An additional requirement that should be imposed on ϕ

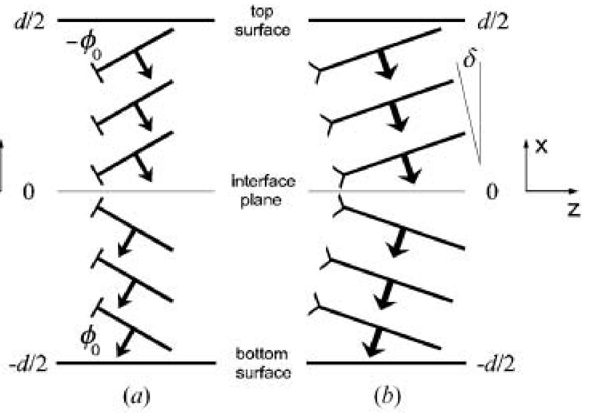

Figure 1. Molecular configuration in unform chevron cells (only one smectic layer in each of the chevron slabs is illustrated). In (a), the smectic layer plane (X–Y) is shown; the symbols→and ⊢ denote projections of the local polarization P_S and the director $\vec{c}$ on the plane (X–Y). In (b), the chevron plane (X–Z) is presented; here, the symbols → and ≻— denote projections of P_S and the director $\vec{n}$ on the plane (X–Z). The pretilt values (in the absence of the external electric field) of the azimuthal angle ϕ are $+\phi_0$ and $-\phi_0$ in the upper and lower chevron slabs, respectively. The smectic layers are inclined about the angle δ.

is that its form derived in the presence of the external alternating electric field should approach a static form as the field frequency tends to zero. Under the above constraints, the solution to (1) can be obtained separately for each of the chevron slabs in the following approximate form [12]

$$\phi_{\pm}(x, t) \approx \mp\phi_0 + b_0^{\pm} + b_1^{\pm} x + F_{\pm}(x)\cos(\omega t - \beta_{\pm}), \tag{5}$$

with

$$F = -\frac{A}{2}\sin(\mp\phi_0 + b_0^{\pm})\cos\beta_{\pm}\left(\frac{d}{2v_{\pm}} \pm \frac{d}{2}x - x^2\right), \tag{6}$$

where

$$b_0^{\pm} = \mp b_1^{\pm}\frac{d}{2}, \tag{7}$$

$$b_1^{\pm} = 2\sqrt{\frac{u_{\pm}}{d}}, \tag{8}$$

and

$$\beta_{\pm} = \arctan\left[\frac{\gamma\omega}{\left(b_1^{\pm}\right)^2}\right]. \tag{9}$$

The parameters b_0^- and b_0^+ can be related to each other by minimizing the interface energy W_{I} with respect to b_0^- for fixed b_0^+, or vice versa. This energy increase is associated with the discontinuity of the average azimuthal angle at the interface plane. For weak external fields, one obtains [12]

$$\varepsilon\varepsilon_0 W_{\mathrm{I}} \Big/ P_S^2 \approx \frac{1}{2}\left(b_0^+ + b_0^-\right)^2 - \frac{1}{4}\left(b_0^+ b_0^-\right)^2. \tag{10}$$

Minimizing W_{I} with respect to b_0^- yields

$$b_0^- \approx -\frac{2b_0^+}{2 - \left(b_0^+\right)^2}. \tag{11}$$

Then, using (7) and (8), one finds

$$v_- \approx \frac{v_+}{1 - \mathrm{d}v_+}. \tag{12}$$

The above approximate relation enables one to reduce the number of anchoring interaction parameters in the description of fluctuations of ϕ.

It follows from (5) and (6) that, as a consequence of the asymmetry of the boundary conditions (3), solutions to the dynamic equation (1) are different for the upper and lower slabs of chevron cells. This implies that the motion of molecules in chevron samples for weak applied fields undergoes two relaxation processes, with different relaxation times. It is also remarkable that, by means of (3), the long time average of $\phi(x, t)$ displays a non-uniform distribution, $\phi_{\pm}(x) = \mp\phi_0 + b_0^{\pm} + b_1^{\pm} x$. Such a distribution of $\bar{\phi}_{\pm}(x)$ through SSFLC samples can be interpreted as a dynamic splay of molecular configuration arising from a reaction of the dynamical viscosity interactions to the action of the applied alternating electric field [12].

3. Theoretical determination of dielectric and optical responses

The contribution to the dielectric susceptibility $\chi(\omega)$ that originates in the azimuthal molecular fluctuations can approximately be characterized by $\phi(x, t)$. Then, using the relations (5)–(9) and (12), one finds [12]

$$\chi(\omega) = \varepsilon'(\omega) + \varepsilon''(\omega)\tan(\omega t), \tag{13}$$

with the dielectric permittivity and the dielectric loss permittivity given by

$$\varepsilon'(\omega) = B\left(\cos^2\beta_+ + \cos^2\beta_-\right), \tag{14}$$

$$\varepsilon''(\omega) = B\left(\tan\beta_+\cos^2\beta_+ + \tan\beta_-\cos^2\beta_-\right) \tag{15}$$

where

$$B = \frac{P_S^2 d}{4\varepsilon_0 v_+ K}\sin^2\phi_0, \tag{16}$$

$$\beta_{\pm} = \tan^{-1}(\omega\tau_{\pm}), \tag{17}$$

and

$$\tau_{\pm} = \frac{\gamma d}{4v_{\pm}}. \tag{18}$$

Accordingly, the dielectric response of chevron SSFLCs is determined by two Debye processes, each of which describes azimuthal motions of molecules in a respective chevron arm. Relaxation times (τ_+ and τ_-) associated with these processes are, in general, different as a consequence of the asymmetry of anchoring interactions at the border surfaces of chevron systems.

The optical response of liquid crystals is usually derived by analysing a field induced distortion of the local dielectric permittivity tensor $\hat{\varepsilon}_{ij}$, $i, j = x, y, z$, in the laboratory frame (associated with a liquid-crystal sample and reflecting its macroscopic symmetry) [1]. This tensor can be determined by transforming the permittivity tensor ε_{mn}, m, $n = 1, 2, 3$, defined in the molecular frame (reflecting molecular symmetry, i.e. being determined by the principal axes of ε_{mn}). As SSFLCs with chevron structure are, in general, biaxial media, the tensor ε_{mn} is assumed here to have a biaxial symmetry, i.e. $\varepsilon_{mn} = \varepsilon_n\delta_{mn}$ with $\varepsilon_1 \neq \varepsilon_2 \neq \varepsilon_3$. The orientation of the local dielectric permittivity ellipsoid (or the molecular frame) in the laboratory frame is described for systems with chevron geometry by three angles: by the smectic tilt θ, by the azimuthal angle ϕ' between the $\vec{c}$ director and the Y axis (see figure 1) and by the layer smectic tilt δ. The angle δ is always less than θ and, in typical cases, takes values from the range 10°–20°. Thus, in the analysis of the optical response of chevron samples, the slant of smectic layers can approximately be ignored by setting $\delta = 0$. Then, the director $\vec{c}$ lies in the smectic plane and, hence, $\phi' = \phi$. In this approximation, the permittivity tensor $\hat{\varepsilon}$ can be expressed by ε applying a double similarity transformation $\hat{\varepsilon} = T_\phi T_\theta \varepsilon T_\theta^{-1} T_\phi^{-1}$, where T_θ and T_ϕ are the Jacobi matrices for rotations of the laboratory frame around the X axis about the angle θ and around the Z axis about the angle ϕ, respectively (note that $\phi = \phi_+$ and $\phi = \phi_-$ for upper and lower chevron slabs). Then, one easily finds

$$\begin{aligned}
\hat{\varepsilon}_{xx}^{\pm} &= \varepsilon_1 + \left(\varepsilon_a + \varepsilon_b \sin^2\theta\right)\sin^2\phi_{\pm},\\
\hat{\varepsilon}_{xy}^{\pm} &= \hat{\varepsilon}_{yx}^{\pm} = \frac{1}{2}\left(\varepsilon_a + \varepsilon_b \sin^2\theta\right)\sin 2\phi_{\pm},\\
\hat{\varepsilon}_{xz}^{\pm} &= \hat{\varepsilon}_{zx}^{\pm} = \frac{1}{2}\varepsilon_b \sin 2\theta \sin\phi_{\pm},\\
\hat{\varepsilon}_{yy}^{\pm} &= \varepsilon_1 + \left(\varepsilon_a + \varepsilon_b \sin^2\theta\right)\cos^2\phi_{\pm},\\
\hat{\varepsilon}_{yz}^{\pm} &= \hat{\varepsilon}_{zy}^{\pm} = \frac{1}{2}\varepsilon_b \sin 2\theta \cos\phi_{\pm},\\
\hat{\varepsilon}_{zz}^{\pm} &= \varepsilon_2 + \varepsilon_b \cos^2\theta,
\end{aligned} \tag{19}$$

where $\hat{\varepsilon}_{ij}^{\pm}$ refer to upper and lower sample arms, $\varepsilon_a = \varepsilon_2 - \varepsilon_1$ and $\varepsilon_b = \varepsilon_3 - \varepsilon_2$. Obviously, the permittivity tensors $\tilde{\varepsilon}^{\pm}$ depend on x through the azimuthal angles $\phi_{\pm} = \phi_{\pm}(x, t)$. However, when the applied electric field is absent, $\phi_{\pm} = \pm\phi_0$ and these tensors are space independent. Thus, according to (19), the unperturbed (by the external electric field) dielectric permittivity tensor $\tilde{\varepsilon}^{(0)}$ is given for the entire chevron cell by

$$\tilde{\varepsilon}^{(0)} = \begin{pmatrix} c_1 & 0 & 0 \\ 0 & c_2 & c_4 \\ 0 & c_4 & c_3 \end{pmatrix} \tag{20}$$

where

$$\begin{aligned}
c_1 &= 2\varepsilon_1 + 2\left(\varepsilon_a + \varepsilon_b \sin^2\theta\right)\sin^2\phi_0,\\
c_2 &= 2\varepsilon_1 + 2\left(\varepsilon_a + \varepsilon_b \sin^2\theta\right)\cos^2\phi_0,\\
c_3 &= 2\varepsilon_2 + 2\varepsilon_b \cos^2\theta,\\
c_4 &= \varepsilon_b \sin^2\theta \cos\phi_0.
\end{aligned} \tag{21}$$

It can easily be verified that, similarly to the zero-field local permittivity tensor ε, the unperturbed, diagonalized effective tensor $\tilde{\varepsilon}^{(0)}$ has, in general, biaxial symmetry. In the presence of the applied electric field, the dielectric permittivity of systems with chevron structure can be characterized by an effective permittivity tensor $\tilde{\varepsilon}$, averaged over both of the chevron slabs. Consequently, putting

$$\phi_{\pm} = \pm\phi_0 + \Delta\phi_{\pm}, \tag{22}$$

where field-induced terms $\Delta\phi_{\pm}$ also include components responsible for the dynamic splay. Inserting $\phi_{\pm}$ into (19), for weak fields one obtains

$$\tilde{\varepsilon} = \begin{pmatrix} c_1 & c_5\langle\Delta\phi\rangle & c_6\langle\Delta\phi\rangle \\ c_5\langle\Delta\phi\rangle & c_2 & c_4 \\ c_6\langle\Delta\phi\rangle & c_4 & c_3 \end{pmatrix} \tag{23}$$

where

$$c_5 = \frac{1}{2}(c_2 - c_1), \tag{24}$$

$$c_6 = \frac{1}{2}c_4, \tag{25}$$

and

$$\langle\Delta\phi\rangle = \frac{2}{d}\int_{-d/2}^{0} \Delta\phi_-(x, t)\,\mathrm{d}x + \frac{2}{d}\int_0^{d/2} \Delta\phi_+(x, t)\,\mathrm{d}x. \tag{26}$$

It can be seen from (20) and (23) that a weak alternating external electric field causes a slight variation of the dielectric permittivity tensor.

The four field-induced elements of $\tilde{\varepsilon}$ are off-diagonal, symmetric. In general, such a modification of the unperturbed permittivity tensor $\tilde{\varepsilon}^{(0)}$ is not equivalent to a transformation of this tensor as a result of a rotation of the laboratory frame around one of its axes. Such an equivalence takes place only if the factors c_5 and c_6 in (23) are specifically related to the elements of $\tilde{\varepsilon}^{(0)}$, e.g. in the manner just determined by (24) and (25). This can easily be checked by rotating the laboratory frame around the Z axis about a small angle ζ (in the case of weak electric fields). Then, the corresponding transformed permittivity tensor $\tilde{\tilde{\varepsilon}} = T_\zeta \tilde{\varepsilon}^{(0)} T_\zeta^{-1}$ with T_ζ being the respective rotation matrix, can be written in the form

$$\tilde{\tilde{\varepsilon}} \approx \begin{pmatrix} c_1 & (c_2 - c_1)\zeta & c_4\zeta \\ (c_2 - c_1)\zeta & c_2 & c_4 \\ c_4\zeta & c_4 & c_3 \end{pmatrix}. \tag{27}$$

Thus, assuming that $\tilde{\varepsilon}$ and $\tilde{\tilde{\varepsilon}}$ are equal, using relations (24) and (25) yields the relation

$$\zeta = \frac{1}{2}\langle\Delta\phi\rangle. \tag{28}$$

Consequently, by means of (23)–(25) and (27), a variation of the dielectric permittivity tensor due to a weak field-induced distortion of the molecular configuration in chevron cells can be identified with a transformation of the unperturbed permittivity tensor, as a consequence of a rotation of the coordination frame around the axis normal to the smectic plane about the angle ζ.

It is clear that the field-generated distortion of configurations of molecules in chevron samples reflects on their optical properties. In particular, the external alternating electric field gives rise to an additional inclination of the light ray passing these systems and causes a modulation of the intensity of the passing light. For small amplitudes of the applied electric field, the inclination of the light ray can be described by the angle ζ, while the ratio of the amplitude of the modulation of the light intensity (after passing a system) to the external electric field is [2]

$$A_{\mathrm{L}} = B_{\mathrm{L}} \frac{\mathrm{d}\zeta}{\mathrm{d}E(t)} = B_{\mathrm{L}} \frac{\langle \Delta\phi \rangle}{2E(t)}, \qquad (29)$$

with the coefficient B_{L} depending on experimental conditions and $E(t)=E\cos(\omega t)$. The average field-generated contribution $<\Delta\phi>$ to the azimuthal angle can be calculated using (26), (22), (5)–(8), (12) and (16) to give

$$\langle \Delta\phi \rangle = \frac{P_S E d}{4v_+ KB} \sin\phi_0 [\varepsilon'(\omega)\cos(\omega t) + \varepsilon''(\omega)\sin(\omega t)]. \qquad (30)$$

Inserting the above equation into (29), one obtains the light intensity modulation

$$A_{\mathrm{L}} = \frac{B_{\mathrm{L}} P_S\, d}{8v_+ KB} \sin\phi_0 [\varepsilon'(\omega) + \varepsilon''(\omega)\tan(\omega t)]. \qquad (31)$$

Thus, the dielectric and optical responses of chevron SSFLCs, characterized respectively by the dynamic dielectric susceptibility $\chi(\omega)$ (13) and by the light intensity modulation A_{L} (31), for collective azimuthal fluctuations of molecules induced by weak sinusoidal electric fields exhibit the same general form of dependence on the field frequency. Consequently, the above theoretical results derived for the dielectric and optical responses are consistent, at least in the case of cooperative molecular processes studied here. Using (16), one can write the ratio of both of the responses in the form

$$\frac{\chi(\omega)}{A_{\mathrm{L}}} = \frac{2P_S \sin\phi_0}{\varepsilon_0 B_{\mathrm{L}}}. \qquad (32)$$

As the quantities χ, A_{L} and B_{L} can be measured, the last relation presents an opportunity to determine the local spontaneous polarization if the pretilt value of the azimuthal angle is known, or vice versa.

4. Experimental results

The consistency of the dielectric and optical responses found theoretically in the previous section is to be verified experimentally, especially because the theoretical results are approximate. For this purpose we used the mixture Felix 015/100 from Clariant, which possesses ferroelectric properties in a broad range of temperature, including room temperature. This material was introduced in its isotropic phase into measuring cells of thickness 5 μm, made by Linkam (UK), and into cells of thickness 12 μm, made by EHC (Japan). Both kinds of measuring cell possess semitransparent ITO (indium tin oxide) electrodes, which enabled simultaneous dielectric and optical experiments to be performed. The electrodes were coated with polymer layers which secured homogeneous alignment of molecules while in the smectic A phase. In this phase (at temperatures between 72°C and 82°C) the molecules are, on average, parallel to the electrodes and the smectic layers are perpendicular to them. In the smectic C* phase, owing to the tilting of molecules with respect to the layer normal, the thickness of smectic layers decreases and the alignment changes in the way shown schematically in figure 1.

To find the correlation between the optical and dielectric responses, both measurements were carried out simultaneously using the experimental setup shown schematically in figure 2. The sample was placed in a thermostatic chamber, the temperature of which was

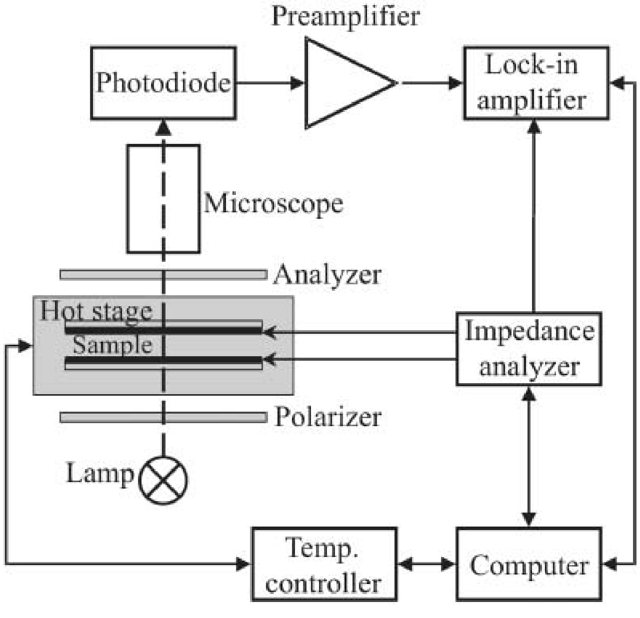

Figure 2. Schematic diagram of the experimental setup for simultaneous dielectric and optical measurements.

controlled using the temperature controller TC 89000-15 made by Digi-Sense with an accuracy better than 0.1 K. The electric permittivity has been measured using the impedance analyser HP 4192A. The measuring voltage of 0.5 V rms was also the source of electro-optic phenomena. The thermostatic chamber with the sample was fixed to the microscope turntable and placed between crossed polarizers. The intensity of light passing the system polarizer–sample–analyser was registered by a photodiode connected with the pre-amplifier. The output of the preamplifier was sent to the lock-in amplifier SR 850 (from Stanford Research, USA). The lock-in amplifier was synchronized with the same voltage that was applied to the sample. The applied measuring instruments allowed for simultaneous measurement of electric permittivity and the depth of light modulation in the frequency range $5\,\mathrm{Hz} < f < 100\,\mathrm{kHz}$ ($f = \omega/2\pi$). To determine the optic axis deviation it was necessary to find the coefficient B_{L} (29). It was determined using the calibration procedure described in [14]. This procedure consists in measuring the change in light intensity after introducing small rotations of the microscope turntable.

Exemplary results are shown in figures 3–8. Figure 3 presents the frequency dependence of real and imaginary parts of ferroelectric contributions to the dielectric susceptibility, χ', χ'', and the frequency dependence of the real and imaginary parts of a field induced deviation of the optic axis, A'_{L}, A''_{L}. The measurement was performed for the Felix mixture in a cell of thickness 5 μm, at 30°C. As figure 3 illustrates, both the dielectric (χ', χ'') and electro-optic (A'_{L}, A''_{L}) responses are very similar within a range of medium frequencies. Note that this observation concerns real as well as imaginary parts of the studied response functions. The resulting correlation of measurement data is even more visible in figure 4, where the real and imaginary parts of the dielectric response are plotted as functions of corresponding parts of the electro-optical response. As shown in figure 4, the dependence of χ on A_{L}, determined experimentally (both for their real and imaginary parts), exhibits a linear form for an intermediate frequency range (roughly given by $1\,\mathrm{kHz} < f < 4\,\mathrm{kHz}$). This clearly demonstrates that the

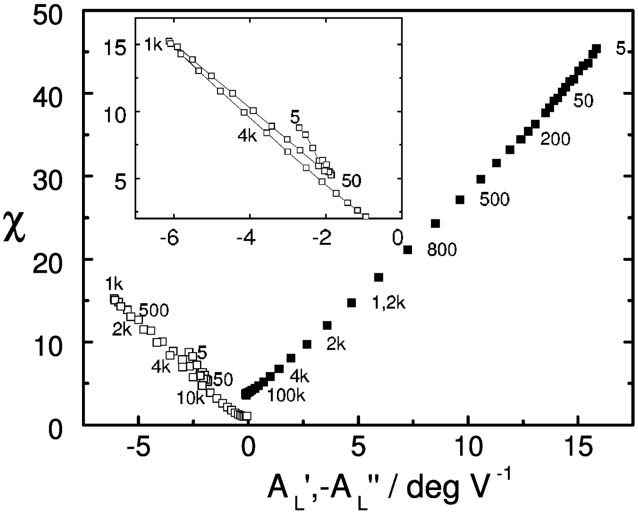

Figure 4. Diagram of the correlation between the complex dielectric susceptibility χ and the complex deviation of the optic axis A_{L} for the experimental data shown in figure 3. For the sake of clarity, negative values are attributed to the imaginary component of the optical response. The measuring frequencies (in Hertz) are shown near some measuring points.

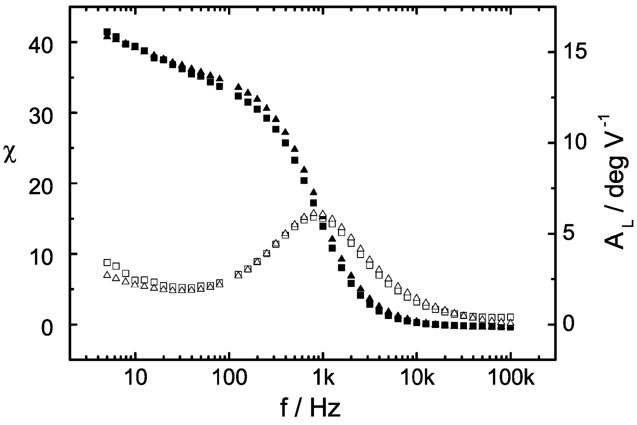

Figure 3. Frequency dependence of the ferroelectric component of the complex dielectric susceptibility χ (squares) and the light modulation depth A_{L} (triangles) for a sample of the mixture Felix 15-100 of thickness 5 μm, at a temperature 30°C. Full symbols and open symbols represent, respectively, real and imaginary parts of the measured quantities.

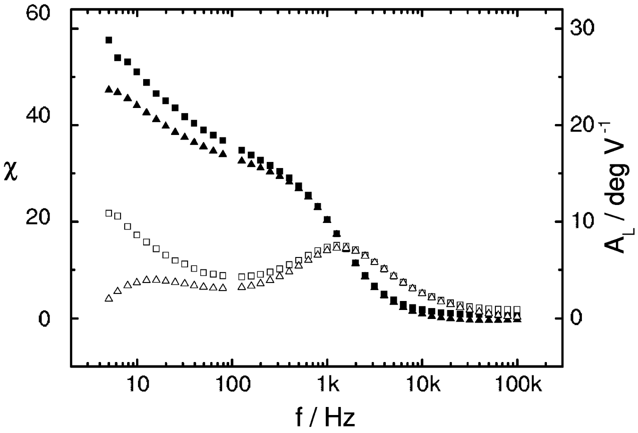

Figure 5. Frequency dependence of the real (full symbols) and imaginary (open symbols) parts of the dielectric susceptibility (squares) and optic axis deviation (triangles) for the Felix sample of thickness 5 μm, at a temperature of 50°C.

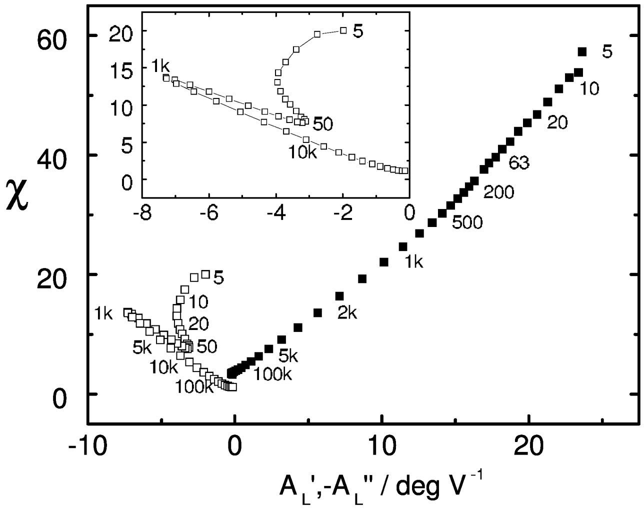

Figure 6. Correlation diagram of dielectric and optical data shown in figure 5.

experimental approaches to study dielectric and optical responses of these systems are equivalent within a medium frequency range (dependent on the specific properties of particular samples), for which fluctuations of azimuthal orientations of molecules dominate the response of chevron liquid-crystal systems to a weak alternating electric field [12]. According to (32), such an equivalence also takes place in the case of the theoretical description of the dielectric and optical responses connected with collective azimuthal motions of molecules in chevron SSFLCs. It is worth noting that the proportionality coefficients connecting the real and imaginary parts of both responses (or the slopes of lines in the plot at medium frequencies) are the same, in agreement with the results of the presented theory.

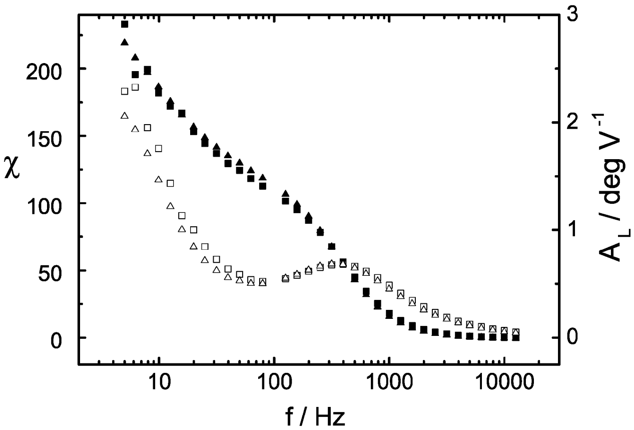

Figure 7. Dielectric susceptibility and optic axis deviation for the Felix sample of 12 μm thickness, at 60°C. The symbols are the same as those used in figures 3 and 5.

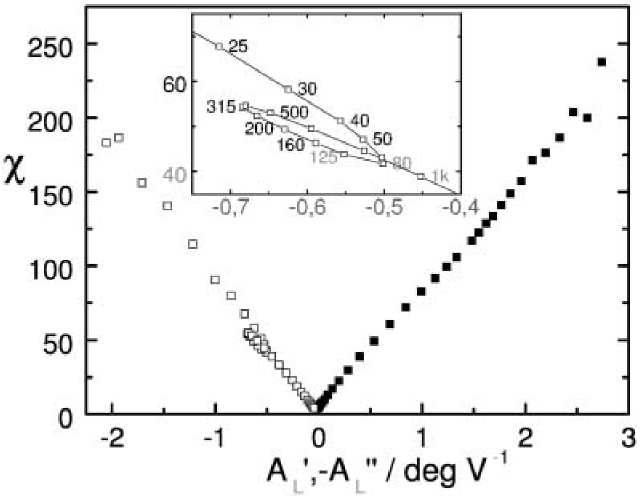

Figure 8. Correlation diagram for the measurement results presented in figure 7.

Closer inspection of figure 4 shows that in the region of relatively low frequencies (below 1 kHz) the dielectric and electro-optic data slightly differ. The deviation from the linear shape of the function $\chi(A_L)$, visible in figures 3 and 4 at low field frequencies (roughly less than 50 Hz), can be explained by the fact that, in contrast to the dielectric response, the optical response is nearly unaffected by ionic currents induced by low-frequency electric fields [3, 11, 15, 16]. The discrepancy between dielectric and optical data caused by ionic currents is more pronounced at higher temperatures, when the concentration and mobility of ions considerably increase. This effect is demonstrated in figures 5 and 6, where the data obtained for the same sample as in figures 3 and 4, but at the temperature 50°C, are plotted. In turn, the deviation from the linearity of $\chi(A_L)$ in a high-frequency region (see figures 3–6) can be attributed to rotations of molecules around their symmetry axes. As is well known, such rotational motions of molecules are uncorrelated and, therefore, affect only the dielectric response of FLCs, especially at high field frequencies [15].

It is also remarkable that another discrepancy between measurement results obtained for dielectric and optical responses of chevron samples may arise at relatively low frequencies, for which the contribution to the dielectric response of SSFLCs due to the dynamics of zigzag defects is significant [12]. Such a discrepancy is seen in figures 4 and 6, especially in the diagram referring to the dielectric loss permittivity, for $50\,\text{Hz} < f < 1\,\text{kHz}$. This inconsistency can easily be explained taking into account that, in contrast to the response of liquid crystals recorded by the dielectric method, the response recorded by the electro-optic approach comes only from some fragments of studied systems. Indeed, sample areas illuminated by light beams used in the optical method are usually smaller than areas of bounding plates of chevron cells and smaller than areas of electrodes to which the voltage is applied. Then, since zigzag defects form macroscopically large objects randomly distributed over chevron samples, the dielectric and optical responses of these samples are affected by the zigzag defects with different, in general, extent.

Similar results have been obtained for the Felix mixture in a cell of thickness 12 μm (see figures 7 and 8). For this system, there also exists a region of field frequencies, for which the dielectric and optical responses are consistent. However, the discrepancy between dielectric and optical data in a region of relatively low frequencies, between 80 Hz and 300 Hz, has a completely different character than in the case of the former sample. This confirms the supposition that the discrepancy seen in figures 5 and 6 within some range of low frequencies, greater than frequencies for which ionic currents give main contributions to the dielectric response, is connected with different averaging of the dielectric and optical responses and with the random formation and distribution of defects in chevron systems.

5. Conclusions

The question of the consistency of dielectric and optical methods in studying the response of SSFLCs of the uniform chevron structure has been tested in the case of collective molecular fluctuations induced by a weak external electric field alternating sinusoidally. The consistency of these approaches has been shown both theoretically and experimentally. However, it must be stressed that the theoretical analysis carried out in this paper has only an approximate character. Approximations applied to analyse the cooperative molecular dynamics have been based mainly on the assumption that surface anchoring interactions are very strong in comparison with intermolecular couplings and with molecular interactions at the interface of chevron slabs (i.e. couplings between molecules adjacent to the chevron plane, from opposite sides of this plane). Another assumption that has been taken here is that the slope of smectic layers in the chevron slabs is very small and can be neglected. This assumption is justifiable when the local polarization takes large values. Then, the applied electric field (alternating or constant) can straighten the smectic layers leading to the quasi-bookshelf structure [6]. Consequently, a good agreement between dielectric and optical response results obtained experimentally may be a consequence of large values of the local polarization in studied samples. Finally, note that the analysis of the consistency and/or inconsistencies between dielectric and optical responses of chevron SSFLCs (and other liquid-crystal systems) can serve as a tool for determining the significance of various field-induced dynamic processes in particular field frequency regions.

References

[1] P. Pierański, E. Guyon, P. Keller, L. Liébert, W. Kuczyński, P. Pierański. *Mol. Cryst. Liq. Cryst.*, **38**, 275 (1977).

[2] W. Kuczyński, J. Hoffmann, J. Małecki. *Ferroelectrics*, **150**, 279 (1993).

[3] W. Kuczyński. Electrooptical studies of relaxation processes in ferroelectric liquid crystals. In *Relaxation Phenomena*, W. Hasse, S. Wróbel (Eds), pp. 422–444, Springer, Berlin (2003).

[4] T.P. Rieker, N.A. Clark, G.S. Smith, D.S. Parmar, E.B. Sirota, C.R. Safinya. *Phys. Rev. Lett.*, **59**, 2658 (1987).

[5] N.A. Clark, T.P. Rieker. *Phys. Rev. A*, **37**, 1053 (1988).

[6] S.T. Lagerwall. *Ferroelectric and Antiferroelectric Liquid Crystals*. Wiley-VCH, Weinheim (1999).

[7] Yu.P. Panarin, Yu.P. Kalmykov, S.T. MacLughadha, H. Xu, J.K. Vij. *Phys. Rev. E*, **50**, 4763 (1994).

[8] M.A. Handschy, N.A. Clark, S.T. Lagerwall. *Phys. Rev. Lett.*, **51**, 47 (1983).

[9] J.E. MacLennan, N.A. Clark, M.A. Handschy, M.R. Meadows. *Liq. Cryst.*, **7**, 753 (1990).

[10] J.E. MacLennan, M.A. Handschy, N.A. Clark. *Liq. Cryst.*, **7**, 787 (1990).

[11] O.E. Kalinovskaya, J.K. Vij, Yu.V. Tretyakov, Yu.P. Panarin, Yu.P. Kalmykov. *Liq. Cryst.*, **26**, 217 (1999).

[12] W. Jeżewski, W. Kuczyński, J. Hoffmann. *Phys. Rev. E*, **73**, 061702 (2006).

[13] M.A. Handschy, N.A. Clark. *Ferroelectrics*, **59**, 69 (1984).

[14] D. Dardas, W. Kuczyński, J. Hoffmann. *Phase Transitions*, **79**, 213 (2006).

[15] F. Gouda, K. Skarp, S.T. Lagerwall. *Ferroelectrics*, **113**, 165 (1991).

[16] S. Sarmento, P. Simeao Carvalho, M. Glogarova, M.R. Chaves, H.T. Nguyen, M.J. Ribeiro. *Liq. Cryst.*, **25**, 375 (1998).